

Influence of thickness on crystallinity in wafer-scale GaTe nanolayers grown by molecular beam epitaxy

Che Jin Bae, Jonathan McMahon, Hermann Detz, Gottfried Strasser, Junsung Park, Erik Einarsson, and D. B. Eason

Citation: *AIP Advances* **7**, 035113 (2017); doi: 10.1063/1.4978776

View online: <http://dx.doi.org/10.1063/1.4978776>

View Table of Contents: <http://aip.scitation.org/toc/adv/7/3>

Published by the [American Institute of Physics](#)

HAVE YOU HEARD?

Employers hiring scientists and engineers trust

PHYSICS TODAY | JOBS

www.physicstoday.org/jobs



Influence of thickness on crystallinity in wafer-scale GaTe nanolayers grown by molecular beam epitaxy

Che Jin Bae,¹ Jonathan McMahon,¹ Hermann Detz,² Gottfried Strasser,² Junsung Park,³ Erik Einarsson,^{3,4} and D. B. Eason^{1,4,a}

¹Shared Instrumentation Laboratories, University at Buffalo, The State University of New York, Buffalo, New York 14260, USA

²Institute for Solid State Electronics, Center for Micro- and Nanostructures, Vienna University of Technology, Vienna, Austria

³Department of Electrical Engineering, University at Buffalo, The State University of New York, Buffalo, New York 14260, USA

⁴Department of Materials Design and Innovation, University at Buffalo, The State University of New York, Buffalo, New York 14260, USA

(Received 10 January 2017; accepted 6 March 2017; published online 15 March 2017)

We grew wafer-scale, uniform nanolayers of gallium telluride (GaTe) on gallium arsenide (GaAs) substrates using molecular beam epitaxy. These films initially formed in a hexagonal close-packed structure (h-GaTe), but monoclinic (m-GaTe) crystalline elements began to form as the film thicknesses increased to more than approximately 90 nm. We confirmed the coexistence of these two crystalline forms using x-ray diffraction and Raman spectroscopy, and we attribute the thickness-dependent structural change to internal stress induced by lattice mismatch with the substrate and to natural lattice relaxation at the growth conditions. © 2017 Author(s). All article content, except where otherwise noted, is licensed under a Creative Commons Attribution (CC BY) license (<http://creativecommons.org/licenses/by/4.0/>). [<http://dx.doi.org/10.1063/1.4978776>]

Since the discovery of graphene in 2004, interest in the field of two-dimensional atomic layered materials has been growing.¹ Due to graphene not having an inherent bandgap, interest moved to transition metal dichalcogenides such as MoS₂, WS₂, WSe₂, and HfS₂, which demonstrate semiconductor properties.² Group III elements have also been found to partner well with Group VI elements to form semiconductors with an inherent bandgap.^{3,4} The intrinsic bandgap in these materials can be tailored by changing the constituent elements and the number of layers. This type of bandgap engineering is of great interest to those developing new devices for photonics, solar energy harvesting, or sensing, but it has proved difficult to obtain uniform, thin layers over large surface areas.^{5,6} Mechanical exfoliation can be performed to obtain these thin layers, but that technique yields small samples and, by its nature, is difficult to scale to large areas. Hence, the availability of wafer-scale, uniformly grown layered materials is desired.

Earlier works regarding GaTe grown by chemical vapor deposition (CVD), critically demonstrated the crystal structure's instability.^{7,8} The hexagonal close-packed crystal structure of GaTe (h-GaTe) tends to be converted to monoclinic (m-GaTe) after annealing at 500 °C, indicating that m-GaTe is the more preferred orientation. This metastable structure was attributed to the fact that every third Ga-Ga bond in the structure changes from out-of-plane position to in-plane position with little gross lattice reorganization and, consequently, the overall layer orientation is retained. The out-of-plane Ga-Ga bond represents the h-GaTe structure, whereas the in-plane Ga-Ga bond represents the m-GaTe. Despite this structural difference, the bond differences between hexagonal and monoclinic crystals are insufficient to affect the electronic properties, as both optical bandgaps fall within the range of 1.7 – 1.75 eV.^{9,10}

In contrast to the other III–VI compounds, GaTe is predicted to be more advantageous when considering optoelectronic applications.^{10,11} Typically, in III–VI layered compounds such as GaS and

^aElectronic mail: dbason@buffalo.edu

GaSe, all Ga–Ga bonds are oriented normal to the layer planes, resulting in an indirect band gap.^{12,13} In m-GaTe, however, one-third of the bonds are parallel to the layer planes, which suggests a direct band gap of 1.7 eV at the Z point of the Brillouin zone. The direct band gap becomes indirect when GaTe is thinned to a monolayer according to theoretical approaches.^{13,14} Therefore, in multilayered GaTe, one can expect improved optical absorption efficiency and enhanced optoelectronic performance compared to a monolayer of GaTe.

Growth of III–VI compounds by molecular beam epitaxy (MBE) has not been demonstrated in the field of layered mono chalcogenides. Now we demonstrate layered growth by MBE, using a custom-built MBE system, including extensive cryogenic shrouding and a cryopump. Initially, to remove the native GaAs oxide on the substrate surface, standard preheating procedures were performed under an arsenic stabilization flux at ~ 600 °C for 15 minutes. The substrate was then cooled to 450 °C for GaTe growth. Growth was also performed at 300 °C, but the crystalline structure formed was found to be more unstable. Solid gallium and tellurium effusion cells were used with a beam equivalent pressure (BEP) flux ratio of Te:Ga of approximately 10:1, providing Te-rich growth conditions. This should cause the layer to exhibit natural p-type conductivity, as it has been suggested that Te-rich growth conditions cause more cation (Ga) vacancies in the GaTe layers which results in p-type conductivity leading to better performing field-effect-transistors and phototransistors based on gated GaTe layers.¹¹ The substrates used in this work were 3-inch diameter (100) semi-insulating GaAs wafers. Figure 1 (a) shows a scanning electron microscope (SEM) cross-sectional image of a sample with a growth time of 210 minutes (167 nm thickness) yielding a growth rate of ~ 8 Å/min.

Figure 1 (b) shows a TEM image, suggesting that a h-GaTe crystalline structure forms and transforms to a m-GaTe crystalline structures growth proceeds. To further demonstrate this, we grew a few layers of GaTe with thicknesses of 4 nm to 16 nm, using the same procedure as discussed above. The blue curve in Fig. 2 (a) reveals the XRD pattern of the 9 nm thick sample, exhibiting only h-GaTe peaks. It has a low signal to noise ratio due to the small film thickness. The red curve

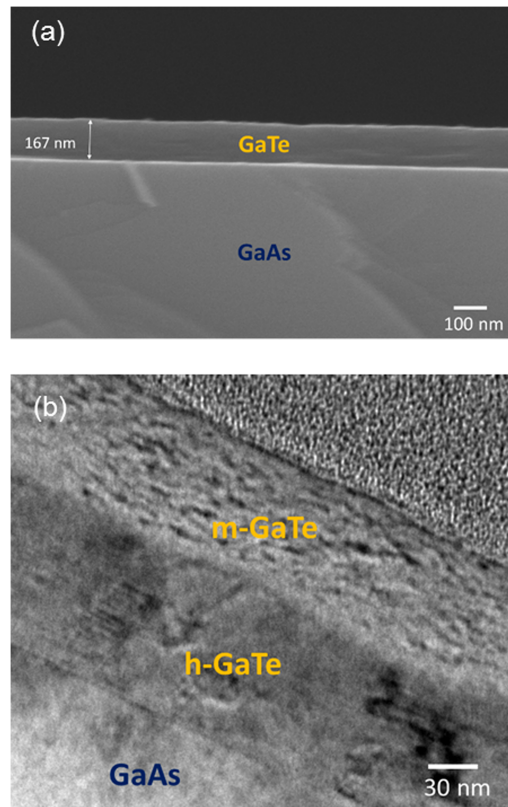


FIG. 1. Cross-section (a) SEM image, and (b) TEM image.

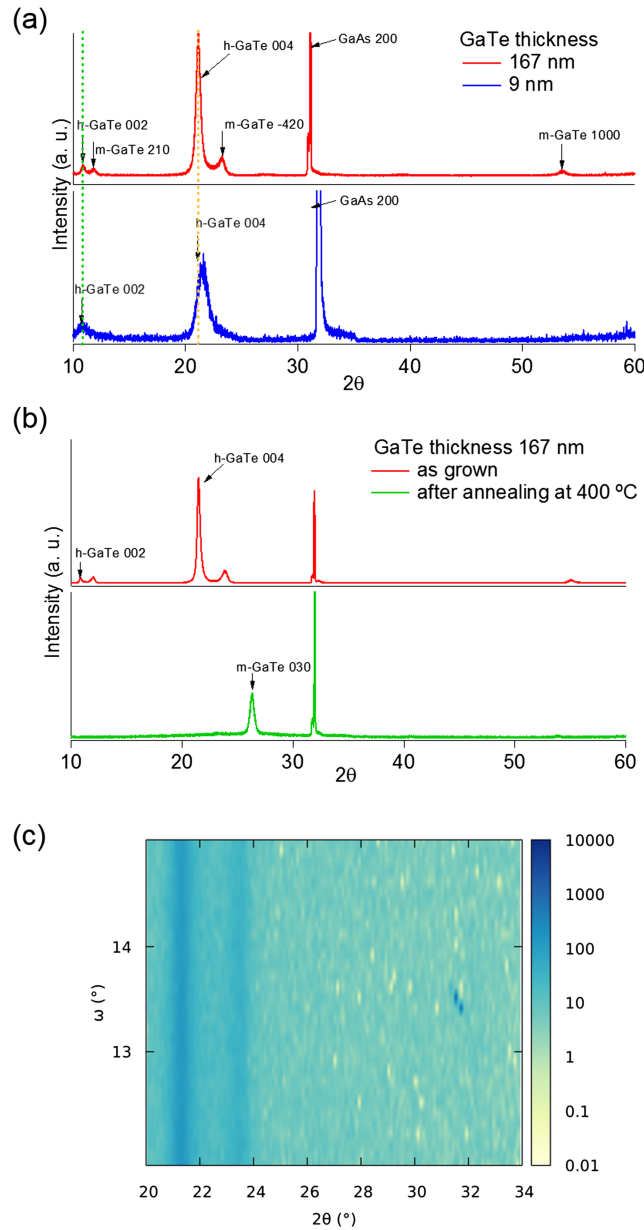


FIG. 2. (a) XRD patterns demonstrate the coexistence of m-GaTe and h-GaTe, (b) XRD pattern before and after 400 °C annealing, (c) reciprocal space map.

in Fig. 2 (a) shows the thicker sample's XRD pattern (167 nm), exhibiting both m-GaTe and h-GaTe peaks. In addition, we confirmed that the GaTe is polycrystalline via a reciprocal space map of the 21.3° h-GaTe, 23.5° m-GaTe and 31.5° GaAs peaks shown in Fig 2 (c). Due to the nucleation on the mismatched GaAs substrates, it was seen that the GaTe formed in a crystalline hexagonal structure almost immediately. The symmetrical h-GaTe ($a=4.1$ Å) crystal structure is more closely matched to the GaAs (100) surface ($a=5.65$ Å) than is the m-GaTe ($a=17.4$ Å, $b=4.08$ Å) crystal structure. The initial stress of the lattice difference between the cubic GaAs (100) surface and the h-GaTe layers (37.8% lattice mismatch) caused the h-GaTe to be the preferred form. As the GaTe layer thickness increases, it relaxes into the more naturally stable state of m-GaTe for these growth conditions.

XRD Peak positions are at 10.52° (0 0 2), and 21.12° (0 0 4) for the h-GaTe peaks, and 11.40° (-2 1 0), and 23.24° (-4 2 0) for the m-GaTe peaks. Only the sample with thickness 167 nm (red

pattern in Fig 2 (a) has a 55.90° peak of m-GaTe. These peaks are in good agreement with other reported h-GaTe properties.^{7,8,15} The red pattern demonstrates a mixed phase of two crystal structures, h-GaTe and m-GaTe. However, the m-GaTe peaks do not appear in the sample of thickness 9 nm (blue pattern) in Fig 2 (a). This is attributed to the fact that the GaTe initially formed in a hexagonal structure, and later transformed into a monoclinic structure. The GaTe structure's instability has been demonstrated in earlier works by annealing samples.⁸ To confirm this hypothesis, we annealed the sample with a thickness of 167 nm, containing both the h-GaTe and m-GaTe layers. We performed a post-growth anneal at 400°C for 5 min under a nitrogen atmosphere in a tube furnace. As seen in Fig 2 (b), the XRD pattern showed both h-GaTe and m-GaTe peaks before annealing. After annealing the sample, shown in the red pattern of Fig 2(b), both the h-GaTe peak at 21.25° and the m-GaTe peak at 23.68° disappeared, and the m-GaTe (0 3 0) peak at 25.88° , a dominant peak of monoclinic GaTe, strongly appeared in the green graph of Fig 2(b). This indicates that the annealing process exerted influence on the Ga-Ga bonds of the sample so that h-GaTe transformed to m-GaTe as discussed above. All traces of the h-GaTe diffraction peaks were gone. Since the annealing process occurred under different conditions than the MBE growth, a different crystalline direction (0 3 0) of the monoclinic GaTe structure is now favored compared to the (-4 2 0) m-GaTe peak that was dominate in the as-grown MBE sample. The reason for this change in peak dominance due to annealing needs further investigation to fully understand the change in GaTe films' structural stress.

Raman scattering was used to investigate the GaTe structural behavior as the sample thickness varied, as shown in Fig 3. Raman peaks at 127 cm^{-1} and 142 cm^{-1} , corresponding to interlayer modes, were observed consistently and without peak variation as thickness increased. In addition to these van

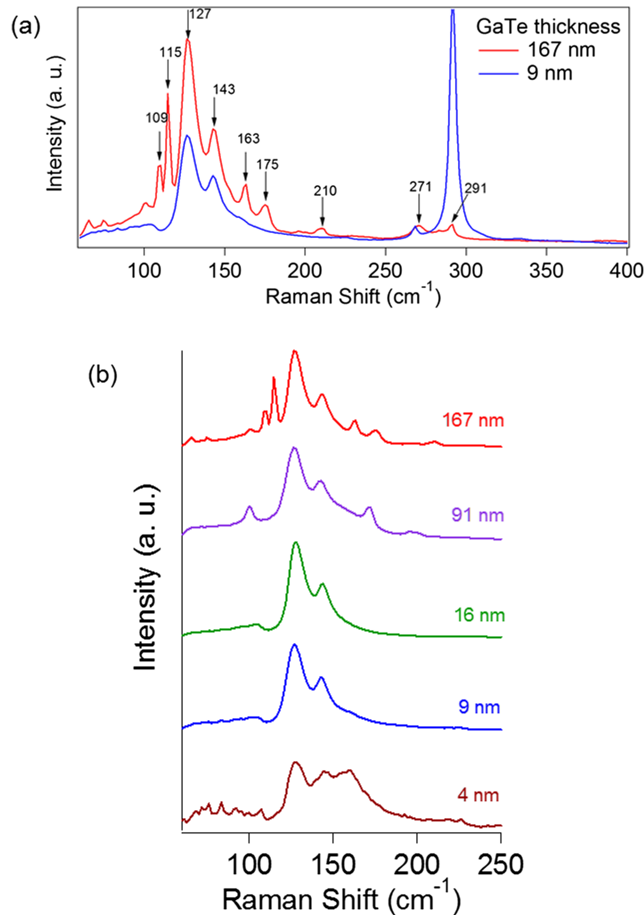


FIG. 3. Raman scattering spectra with an excitation wavelength of 514 nm (a) comparison of thin and thick GaTe nanolayers, and (b) thickness dependence.

der Waals interactions, lateral vibration modes including 109, 115, 163, 175, 210, 271, and 291 cm^{-1} were also observed when the thickness was >91 nm and continued to appear as thickness increased. These additional modes have been demonstrated to be representative of monoclinic GaTe via bulk single crystal growth.^{16–18} This indicated that sample thickness was strongly related to the transition from h-GaTe to m-GaTe. We note that the bulk properties of GaTe in terms of Raman peaks are critical at the thickness of 91 nm. In a recent discussion regarding the oxidation effect of GaTe in air, the van der Waals interactions were affected by surface aging, attributed to the formation of GaTe-O₂, GaTe-OH, and GaTe-H₂O bonds.¹⁹

In conclusion, we employed MBE to grow large area, uniform thickness nanolayers of GaTe on GaAs (001) substrates with thicknesses ranging from 4 to 167 nm. Detailed characterization using cross-sectional TEM, XRD, and Raman scattering exhibited an initial layer of h-GaTe, which later transitioned to a m-GaTe structure. The instability of h-GaTe was demonstrated via an XRD pattern shift towards m-GaTe during post-growth annealing. In contrast, GaSe is a related and stable material system.^{5,6} Multilayers of GaSe and GaTe could be proposed to help stabilize the GaTe. We noted that Raman peaks had a thickness dependence, and that m-GaTe peaks were dominant for thicknesses greater than 91 nm. Future works are needed to verify the relationship between changes caused by surface oxidation and the m-GaTe transition due to lattice mismatch.

We appreciate the TEM images provided by Dr. Yueling Qin of the Center for Materials Informatics (CMI) at the University at Buffalo.

- ¹ K. S. Novoselov, A. K. Geim, S. V. Morozov, D. Jiang, Y. Zhang, S. V. Dubonos, and A. A. Firsov, *Science* **306**, 666 (2004).
- ² Q. H. Wang, K. Kalantar-Zadeh, A. Kis, J. N. Coleman, and M. S. Strano, *Nat. Nanotechnol.* **7**, 699 (2012).
- ³ O. Z. Alekperov, M. O. Godjaev, M. Z. Zarbaliev, and R. A. Suleimanov, *Solid State Commun.* **77**, 65 (1991).
- ⁴ H. Ho and S. L. Lin, *J. Appl. Phys.* **100**, 083508 (2006).
- ⁵ S. Lei, L. Ge, Z. Liu, S. Najmaei, G. Shi, G. You, J. Lou, R. Vajtai, and P. M. Ajayan, *Nano Lett.* **13**, 2777 (2013).
- ⁶ X. Li, M. W. Lin, A. A. Puretzky, J. C. Idrobo, C. Ma, M. Chi, M. Yoon, C. M. Rouleau, I. I. Kravchenko, D. B. Geohegan, and K. Xiao, *Sci. Rep.* **4**, 5497 (2014).
- ⁷ S. A. Semelitov and V. A. Vlasov, *Sov. Phys. Crystallogr.* **8**, 704 (1964).
- ⁸ E. G. Gillan and A. R. Barron, *Chem. Mater.* **9**, 3037 (1997).
- ⁹ J. F. Sanchez-Royo, J. Pellicer-Porres, A. Segura, V. Munoz-Sanjoseet, G. Tobias, P. Ordeedjeon, E. Canadell, and Y. Huttel, *Phys. Rev. B* **65**, 115201 (2002).
- ¹⁰ L. Fucai, H. Simotani, H. Shang, T. Kanagasekaran, V. Zolyomi, N. Drummond, V. I. Fal'ko, and K. Tanigaki, *ACS Nano* **8**, 752 (2014).
- ¹¹ Z. Wang, K. Xu, Y. Li, X. Zhan, M. Safdar, Q. Wang, F. Wang, and J. He, *ACS Nano* **8**, 4859 (2014).
- ¹² C. H. Ho and S. L. Lin, *J. Appl. Phys.* **100**, 083508 (2006).
- ¹³ H. L. Zhang and R. G. Hennig, *Chem. Mater.* **25**, 3232 (2013).
- ¹⁴ V. Zolyomi, N. D. Drummond, and V. I. Fal'ko, *Phys. Rev. B* **87**, 195403 (2013).
- ¹⁵ P. M. Julien-Pouzol, S. Jaulmes, M. Guittard, and F. Alapini, *Acta Cryst. B* **35**, 2848 (1979).
- ¹⁶ G. B. Abdullaev, L. K. Vodopyanov, K. R. Allakhverdiev, L. V. Golubev, S. S. Babaev, and E. Y. Salaev, *Solid State Commun.* **31**, 1851 (1979).
- ¹⁷ J. C. Irwin, B. P. Clayman, and D. G. Mead, *Phys. Rev. B* **19**, 2099 (1979).
- ¹⁸ A. Yamamoto, A. Syouji, T. Goto, E. Kulatov, K. Ohno, Y. Kawazoe, K. Uchida, and N. Miura, *Phys. Rev. B* **64**, 035210 (2001).
- ¹⁹ J. J. Fonseca, S. Tongay, M. Topsakal, A. R. Chew, A. J. Lin, C. Ko, A. V. Luce, A. Salleo, J. Wu, and O. D. Dubon, *Adv. Mater.* **28**, 6465 (2016).